www.nature.com/aps

Acta Pharmacologica Sinica

ARTICLE

14-Deoxygarcinol improves insulin sensitivity in high-fat diet-induced obese mice via mitigating NF-κB/Sirtuin 2-NLRP3-mediated adipose tissue remodeling

Jia-li Chen[1], Zhe-ling Feng[1,2], Fei Zhou[1], Ruo-han Lou[1], Cheng Peng[3], Yang Ye[2] and Li-gen Lin[1,4]

Interleukin (IL)-1β is a culprit of adipose tissue inflammation, which in turn causes systematic inflammation and insulin resistance in obese individuals. IL-1β is mainly produced in monocytes and macrophages and marginally in adipocytes, through cleavage of the inactive pro-IL-1β precursor by caspase-1, which is activated via the NLRP3 inflammasome complex. The nuclear factor-κB (NF-κB) transcription factor is the master regulator of inflammatory responses. Brindle berry (*Garcinia cambogia*) has been widely used as health products for treating obesity and related metabolic disorders, but its active principles remain unclear. We previously found a series of polyisoprenylated benzophenones from brindle berry with anti-inflammatory activities. In this study we investigated whether 14-deoxygarcinol (DOG), a major polyisoprenylated benzophenone from brindle berry, alleviated adipose tissue inflammation and insulin sensitivity in high-fat diet fed mice. The mice were administered DOG (2.5, 5 $mg \cdot kg^{-1} \cdot d^{-1}$, i.p.) for 4 weeks. We showed that DOG injection dose-dependently improved insulin resistance and hyperlipidemia, but not adiposity in high-fat diet-fed mice. We found that DOG injection significantly alleviated adipose tissue inflammation via preventing macrophage infiltration and pro-inflammatory polarization of macrophages, and adipose tissue fibrosis via reducing the abnormal deposition of extracellular matrix. In LPS plus nigericin-stimulated THP-1 macrophages, DOG (1.25, 2.5, 5 μM) dose-dependently suppressed the activation of NLRP3 inflammasome and NF-κB signaling pathway. We demonstrated that DOG bound to and activated the deacetylase Sirtuin 2, which in turn deacetylated and inactivated NLRP3 inflammasome to reduce IL-1β secretion. Moreover, DOG (1.25, 2.5, 5 μM) dose-dependently mitigated inflammatory responses in macrophage conditioned media-treated adipocytes and suppressed macrophage migration toward adipocytes. Taken together, DOG might be a drug candidate to treat metabolic disorders through modulation of adipose tissue remodeling.

Keywords: 14-deoxygarcinol; adipose tissue inflammation; insulin resistance; interleukin-1β; NLRP3 inflammasome; Sirtuin 2

Acta Pharmacologica Sinica (2023) 44:434–445; https://doi.org/10.1038/s41401-022-00958-8

INTRODUCTION

Obesity has nearly tripled in the past several decades throughout the world, both children and adults [1], causing an explosion of obesity-related metabolic diseases, such as fatty liver, cardiovascular diseases and type 2 diabetes [2–4]. Growing evidence has indicated that adipose tissue inflammation plays an essential role in obesity-induced metabolic disorders [5, 6]. Increased macrophage infiltration and pro-inflammatory polarization of macrophages result in adipose tissue inflammation, which in turn induces systematic inflammation and insulin resistance in obese subjects [7]. Interleukin (IL)-1β, one of the principal inflammatory cytokines that affect nearly every cell type and mediate inflammation in a variety of tissues, is produced by cleavage of the inactive pro-IL-1β precursor by caspase-1 via the NLRP3 inflammasome complex [8]. The nuclear factor-κB (NF-κB) signaling pathway has long been considered as the master regulator of pro-inflammatory responses [9]. Activation of the NLRP3 inflammasome is thought to be regulated at both the transcriptional (priming) and post-translational (activation) levels. The priming signal activates NF-κB via Toll-like Receptor 4 to induce the transcription of NLRP3 and pro-IL-1β [10]. When activated, NLRP3 binds to the adapter protein apoptosis associated speck-like protein containing a caspase recruitment domain, resulting in the cleavage of pro-caspase-1, an indispensable step to produce and release mature IL-1β [11]. IL-1β is considered as a culprit to induce adipose tissue inflammation and impair insulin signaling in obese mice and diabetic rats [12]. Thus, suppression of NLRP3-caspase-1-mediated IL-1β production in macrophages is vital to ameliorate adipose tissue inflammation and improve insulin sensitivity [13].

Natural products have become a promising alternative to treat obesity-associated metabolic diseases due to their efficiency and safety. Brindle berry (*Garcinia cambogia*) is one of the most medicinally essential members of the family Clusiaceae [14]. In many Asian countries, brindle berry is commonly used as a flavoring agent, food preservative and food-bulking agent [15]. In addition,

[1]State Key Laboratory of Quality Research in Chinese Medicine, Institute of Chinese Medical Sciences, University of Macau, Macao, China; [2]State Key Laboratory of Drug Research and Natural Products Chemistry Department, Shanghai Institute of Materia Medica, Chinese Academy of Sciences, Shanghai 201203, China; [3]State Key Laboratory of Southwestern Chinese Medicine Resources, School of Pharmacy, Chengdu University of Traditional Chinese Medicine, Chengdu 610075, China and [4]Department of Pharmaceutical Sciences, Faculty of Health Sciences, University of Macau, Macao, China
Correspondence: Li-gen Lin (ligenl@um.edu.mo)

Received: 4 March 2022 Accepted: 12 July 2022
Published online: 9 August 2022

brindle berry is a traditional remedy for the treatment of bowel complaints, intestinal parasites and rheumatism [14, 16]. Pharmacological studies showed that the extracts and compounds from brindle berry possess a wide spectrum of bioactivities, including anti-obesity, anti-diabetes, anti-ulcer, and anti-inflammation [17, 18]. In our previous study, a series of polyisoprenylated benzophenones were isolated from brindle berry; and 4.8-*epi*-uralione F was found to suppress the activation of NF-κB signaling pathway to exert anti-inflammatory effect [19]. 14-Deoxygarcinol (DOG), a major polyisoprenylated benzophenone from brindle berry, exhibited potent inhibitory effect against the production of nitric oxide (NO) in lipopolysaccharide (LPS)-induced RAW264.7 macrophages in our preliminary study. However, the roles of DOG in alleviating adipose tissue inflammation and improving insulin sensitivity remain unclear. Herein, we investigated the role of DOG in alleviating adipose tissue inflammation in high-fat diet (HFD)-induced obese mice and uncovered the underlying mechanisms.

MATERIALS AND METHODS

Reagents

DOG was dissolved in dimethyl sulfoxide (DMSO) at a concentration of 10 mM as the stock solution and stored at −20 °C. 3-(4,5-Dimethyl-2-thiazolyl)-2,5-diphenyltetrazolium bromide (MTT), LPS, dexamethasone (DEX), 1-methyl-3-isobutylxanthine (IBMX), insulin, tumor necrosis factor-α (TNF-α), Tween-20, PEG400, and DMSO were purchased from Sigma-Aldrich (St. Louis, MO, USA). Radio immunoprecipitation assay buffer (RIPA) was obtained from Beyotime Biotechnology (Shanghai, China). Dulbecco's modified Eagle's medium (DMEM), fetal bovine serum (FBS), penicillin-streptomycin (P/S), phosphate-buffered saline (PBS), and 0.25% trypsin-EDTA were purchased from Gibco (Carlsbad, CA, USA). Calf serum (CS) was provided by HyClone (Logan, UT, USA). BCA Protein Assay Kit and TRIzol RNA extraction reagent were acquired from Thermo Fisher Scientific (Grand Island, NY, USA).

Isolation and purification of DOG

The fruits of *G. cambogia* were collected in New Delhi, India. The air-dried and powdered fruits of *G. cambogia* (15 kg) were extracted with 95% ethanol (30 L) for three times, each 24 h. The alcohol extract (5.4 kg) was suspended in 15 L water and extracted with petroleum ether (PE, 5 L × 3 times), chloroform (5 L × 3 times) and ethyl acetate (EtOAc, 5 L × 3 times) successively. Then, the chloroform soluble fraction (700 g) was subjected to column chromatography (CC) over macroporous resin D101 eluting with ethanol/water (0:1, 3:7, 6:4, 9:1, 1:0, *v/v*), to afford three fractions, D30, D60 and D90. The D90 fraction (82.77 g) was subjected CC over silica gel eluting with PE/acetone (15:1, 12:1, 9:1, 7:1, 5:1, 3:1, 2:1,1:1, *v/v*) to afford seven fractions (A–G). Fraction C (1.01 g) was subjected to CC over Sephadex LH-20 eluting with chloroform/methanol (1:1, *v/v*) to afford four fractions CA–CD. Fraction CD (0.70 g) was purified by reversed-phase semi-preparative high performanceliquid chromatography (CH_3CN/H_2O, 1:1–1:0, *v/v*; 40 min, flow rate 10 mL/min, photodiode array detector 254 nm, a Shimadzu LC-20AP instrument) to yield compound DOG.

Animal experimental procedure

Male C57BL/6J mice were randomly separated into two groups and fed with a regular chow diet (calorie 2.35 kcal/g) and a 45% HFD (calorie 4.5 kcal/g, Trophic Animal Feed High-Tech Co., Nantong, China), respectively, for 10 weeks. Subsequently, the regular chow diet-fed mice were further separated into two groups and intraperitoneally injected with 5 mL/kg PEG 400 solution (RD, PEG 400/0.9% saline, 6:4, *v/v*) and the same volume of DOG solution (RD-H, 5 mg/kg DOG, 0.5 mg/mL dissolved in PEG 400 solution), respectively. The HFD-fed mice were further separated into three groups and intraperitoneally injected with 5 mL/kg PEG 400 solution (HFD), low dosage DOG solution (HFD-L, 2.5 mg/kg DOG, 0.25 mg/mL dissolved in PEG 400 solution) and high dosage of DOG solution (HFD-H, 5 mg/kg DOG, 0.5 mg/mL dissolved in PEG 400 solution), respectively. The mice were injected once a day for 4 weeks. Body weight and food intake were monitored every 5 days. Blood samples were collected from tail vein after 16 h fasting and centrifuged at 1200 × *g* for 10 min at room temperature. Serum was aliquoted and stored at −80 °C. Epididymal white adipose tissues (eWAT) were dissected. One part of the eWAT was fixed in 4% paraformaldehyde, and the rest of the tissues was quickly frozen in liquid nitrogen and preserved at −80 °C for subsequent studies.

Glucose tolerance tests (GTTs) and insulin tolerance tests (ITTs)

GTTs and ITTs were performed as described previously [20]. The basal blood glucose level was measured using the OneTouch Ultra blood glucose meter and LifeScan test strips. For the GTTs, after 16 h fasting, the mice were intraperitoneally injected a glucose solution (Sigma-Aldrich) at a dose of 1.5 g/kg body weight. For the ITTs, after 6 h fasting, the mice were administered by an intraperitoneal injection of human insulin (Eli Lilly, Indianapolis, IN, USA) at a dose of 1.0 U/kg body weight. Then, the tail blood glucose levels were measured at 15, 30, 60, 90, and 120 min after injections.

Homeostasis model assessment of basal insulin resistance

Plasma insulin was measured using the insulin assay kit (Sigma-Aldrich) according to the manufacturer's instructions. The homeostasis model assessment of basal insulin resistance (HOMA-IR) index was calculated as following: fasting serum glucose × fasting serum insulin/14.1, to assess insulin resistance [21].

Lipid profiles

The levels of total cholesterol (TC), triglycerides (TG), high-density lipoprotein cholesterol (HDL), and low-density lipoprotein cholesterol (LDL) in mice serum were determined by using commercial kits (Nanjing Jiancheng Bioengineering Institute, Nanjing, China).

Determination of cytokines

The cytokines in cell medium, mice serum and tissue lysates were determined by using commercial ELISA kits (Neobioscience Technology Co., Ltd., Shenzhen, China), following the manufacturer's instruction. NO production in cell medium was determined using Griess reagent (Sigma-Aldrich).

Histological analysis

The eWAT was fixed in 10% buffered formalin, and then embedded in paraffin. H&E staining was performed according to standard experimental procedures.

Immunofluorescence staining

Immunofluorescence staining was performed as described previously [20]. After deparaffinization and rehydration, paraffin-wax-embedded eWAT sections were pretreated with 10 mM citric acid (pH 6.0) and heated in a water bath to recover antigenicity, followed by block with 10% BSA in PBS for 1 h at room temperature to avoid unspecific binding. The eWAT sections were stained with primary antibodies against perilipin 1 (1:100 dilution, Abcam, Cambridge, UK) and F4/80 (1:100 dilution, Santa Cruz Biotechnology, Santa Cruz, CA, USA) for 24 h at 4 °C. The sections were washed and subsequently incubated with anti-rabbit or anti-mouse IgG secondary antibodies (1:1000 dilution, Thermo Fisher) for 30 min at room temperature. THP-1 cells were fixed in 4% paraformaldehyde. Then the specific primary antibody (1:100 dilution) was added and incubated at 4 °C for 24 h and then washed twice with TBST buffer, followed by incubating with the corresponding secondary antibody (1:1000 dilution, Thermo Fisher) for 30 min at room temperature. The fluorescent images were captured by a confocal microscope (Olympus, Tokyo, Japan).

Cell culture

Mouse-derived RAW264.7 macrophages were obtained from the American Type Cell Collection (ATCC, Manassas, VA, USA) and cultured in DMEM with 10% FBS and maintained in a humidified incubator with 5% CO_2 at 37 °C. Human-derived THP-1 macrophages were obtained from ATCC and maintained in RPMI-1640 medium supplemented with 10% FBS. THP-1 cells were stimulated by phorbol 12-myristate 13-acetate (PMA, 100 ng/mL, Sigma-Aldrich) for 12 h to differentiate into macrophages.

3T3-L1 preadipocytes were obtained from ATCC and maintained in DMEM containing 10% CS and 1% P/S. Cells were differentiated into adipocytes as reported previously [20]. Briefly, 2 days post-confluent 3T3-L1 preadipocytes were stimulated with DMEM supplemented with 10% FBS, 1 μM Dex, 0.5 mM IBMX and 5 μg/mL insulin for 2 days. Cells were subsequently cultured in maintaining medium (DMEM supplemented with 10% FBS and 5 μg/mL insulin) for 6 days. The medium was changed every other day. The fully differentiated 3T3-L1 cells was checked by microscopic observation.

Macrophage-adipocyte co-culture

Macrophage-adipocyte co-culture was performed as described previously [22]. THP-1 macrophages were treated with or without 5 μM DOG for 12 h and 5 μM AGK2, a known SIRT2 inhibitor (Sigma-Aldrich), for 6 h. Subsequently, the cells were stimulated with LPS (1 μg/mL) for 4 h and then nigericin (5 nM) for 1 h. After removing the medium, THP-1 macrophages were rinsed twice with RPMI-1640 medium and then incubated in RPMI-1640 medium (serum free, 0.2% endotoxin and fatty acid-free BSA) for 24 h. The medium was harvested and centrifuged at 4000 × *g* for 10 min, and the supernatant was collected as macrophage conditioned media (CM). The fully differentiated 3T3-L1 adipocytes were incubated with migration medium (serum free, 0.2% endotoxin and fatty acid-free BSA in DMEM) for 24 h. Subsequently, the adipocytes were incubated with macrophage CM for 24 h, and then harvested for further studies.

For macrophage migration assay, transwell inserts with an 8 μm membrane pore size (Millipore, Bedford, MA, USA) were used. The fully differentiated 3T3-L1 adipocytes were incubated with migration medium for 24 h. The medium was harvested and centrifuged at 4000 × *g* for 10 min, and the supernatant was collected as adipocyte CM. THP-1 macrophages were seeded onto the inserts at a density of 5×10^4 cells per well and treated with or without 5 μM DOG for 12 h and 5 μM AGK2 for 6 h. Then, the macrophages were co-cultured with adipocyte CM for 4 h at 37 °C. The macrophages in the lower compartment were fixed with 4% formaldehyde for 20 min, stained with DAPI, and counted as described previously [23].

Cell viability

Cell viability was determined by MTT assay as described previously [24]. RAW264.7 macrophages, THP-1 macrophages and 3T3-L1 preadipocytes were seeded in 96-well plates at a density of 1×10^4 cells per well. Cells were treated with different concentrations of DOG for 24 h. Then cell viability was determined by incubation with DMEM or RPMI-1640 medium containing MTT (1 mg/mL) for 4 h, followed by dissolving the formazan crystals with DMSO. The absorbance at 570 nm was measured by a SpectraMax M5 microplate reader (Molecular Devices, CA, USA). The calculation equation for relative cell viability was as following: cell viability (%) = (As − A0)/(Ac − A0) × 100%, where As, A0 and Ac were the absorptions of test sample, blank control and negative control (DMSO).

Protein harvest from cell culture medium

THP-1 cell culture media were collected and centrifuged at 15,000 × *g* for 10 min at 4 °C. Then the supernatant was transferred to a new tube and mixed with 700 μL methanol and 175 μL chloroform. The mixture was centrifuged at 21,000 × *g* for 10 min at 4 °C after sit for 5 min at room temperature. The liquid portion in the mixture was removed, and the white intermediate layer was collected and washed by 700 μL methanol. Then the protein sample was dissolved in 2% SDS sample buffer for Western blotting analysis.

Western blotting analysis

Western blotting was performed as described previously [23, 25]. 3T3-L1 adipocytes, THP-1 macrophages and eWAT were lysed with RIPA lysis buffer. Protein concentration was determined using a BCA Protein Assay Kit. An equal number of proteins (20–30 μg) were separated by SDS-PAGE, transferred to PVDF membranes, blocked with 5% nonfat milk in TBST buffer (100 mM NaCl, 10 mM Tris-HCl, pH 7.5 and 0.1% Tween-20) for 2 h at room temperature, and incubated with specific primary antibodies (Supplementary Table S1) overnight at 4 °C. After washing with TBST thrice, a corresponding horseradish peroxidase conjugated secondary antibody was added and incubated for 2 h at room temperature. Signals were detected using a SuperSignal West Femto Maximum Sensitivity Substrate kit (Thermo Fisher) and visualized using the ChemiDoc MP Imaging System (Bio-Rad, Hercules, CA, USA).

Cellular thermal shift assay (CETSA)

THP-1 cells were pretreated with or without 5 μM DOG for 12 h. The cells were lysed by RIPA lysis buffer. The cell lysates were incubated in ice for 10 min, and then centrifuged at 12,000 × *g* for 15 min at 4 °C. The protein concentration was adjusted to 2 μg/μL using RIPA lysis buffer. Then 50 μL cell lysates were transferred to new tubes and heated for 5 min at different temperatures (50–90 °C) using a thermal cycler. After incubation in ice for 10 min, soluble proteins were obtained by centrifuging at 12,000 × *g* for 20 min at 4 °C and analyzed by Western blotting analysis.

SIRT2 deacetylating activity

The effects of DOG (5 μM) and AGK2 (5 μM) on SIRT2 deacetylating activity were measured with a SIRT2 Direct Fluorescent Screening Assay Kit (Cayman Chemical, Ann Arbor, Michigan, USA) according to the manufacturer's instruction. The fluorescence intensities were measured with a microplate fluorimeter (excitation wavelength = 360 nm, emission wavelength = 460 nm). All values were represented as percentages of the control group.

Co-immunoprecipitation

THP-1 cell lysates were mixed with the indicated antibody and subsequently 20 μL protein A/G-agarose beads (Santa Cruz Biotechnology), and then incubated on a rotator for 4 h at 4 °C. The beads were washed thrice with PBS and then thrice with lysis buffer supplemented with complete mini-protease inhibitor cocktail. Bound proteins were boiled in sample preparation buffer for 10 min and analyzed by Western blotting analysis.

Real-time RT-PCR

Isolation of total RNA from cells and eWAT was performed using the TRIzol Reagent (Invitrogen, Carlsbad, CA, USA), following the manufacturer's instruction. RNA (1 μg) was reversely transcribed into complementary cDNA using the SuperScript III First Strand Synthesis System (Thermo Fisher). The qPCR experiments were conducted on a Step-One plus real-time PCR System using SYBR green PCR Master Mix (Thermo Fisher) with gene specific primers (Supplementary Table S2). Relative mRNA levels were calculated using $2^{-\Delta\Delta Ct}$ method. The 18S RNA was used as a housekeeping gene.

Statistical analysis

All data were analyzed using GraphPad Prism 7.0 (GraphPad Software, San Diego, CA, USA). All experimental data were

expressed as mean ± SEM, and the sample size for each experiment corresponds to three biological replicates. Significant differences between groups were determined using a one-way analysis of variance with Dunnet's multiple comparisons test, considering $P < 0.05$ as a statistically significant difference.

RESULTS

DOG alleviates insulin resistance and hyperlipidaemia in HFD-challenged mice

Although the fruits of *G. cambogia* have been widely used to treat inflammation related diseases, the anti-inflammatory property of polyisoprenylated benzophenones from the aforementioned herbal materials was seldom investigated. To fill this gap, we evaluated the anti-inflammatory effect of the major polyisoprenylated benzophenones on LPS-treated RAW264.7 macrophages. Among them, DOG (Fig. 1a) did not show obvious cytotoxicity on RAW264.7 cells up to 10 μM, and showed the most potent inhibitory effect against NO production with an IC_{50} value of 2.37 ± 0.08 μM (Supplementary Fig. S1a–c). Additionally, DOG suppressed the expression of inducible NO synthase (iNOS) and the levels of inflammatory cytokines, including TNF-α, IL-6 and monocyte chemoattractant protein-1 (MCP-1, Supplementary Fig. S1d–g). To evaluate the role of DOG in alleviating adipose tissue inflammation, HFD-challenged obese mice were recruited. Either high or low dosage of DOG did not obviously affect body weight (Supplementary Fig. S2a) or food intake (Supplementary Fig. S2b) compared to those of HFD-fed mice.

GTTs and ITTs were performed to characterize whether DOG could improve systemic insulin sensitivity. During GTTs, the HFD-fed mice showed an impaired glucose disposal rate compared with the RD-fed mice, while high dosage of DOG treatment obviously improved the glucose clearance rate in HFD-fed mice (Fig. 1b). Consistently, the ITT results indicated that HFD feeding decreased insulin sensitivity, and either high or low dosage of DOG treatment greatly improved insulin sensitivity in HFD-fed mice (Fig. 1c). After 16 h fasting, the blood glucose level and serum insulin level were greatly higher in HFD-fed mice, compared with those of the RD-fed mice; and high dosage of DOG treatment obviously reduced blood glucose and serum insulin levels (Fig. 1d, e). Interestingly, DOG treatment totally abolished the effects of HFD feeding back to the levels of RD group in GTTs, ITTs, the fasting blood glucose levels and serum insulin levels. The HOMA-IR index indicated that high dosage DOG treatment improved insulin sensitivity in HFD-fed mice (Fig. 1f). Furthermore, the levels of serum lipid parameters were evaluated. Compared to the HFD-fed mice, either low or high dosage of DOG treatment significantly reduced the serum levels of TC, TG and LDL, and obviously increased the serum level of HDL (Fig. 1g). Compared to the RD-fed mice, low or high dosage of DOG treatment cannot restore the serum levels of TC, TG, LDL and HDL under HFD challenge (Fig. 1g). Taken together, DOG ameliorates insulin resistance and hyperlipidaemia in HFD-fed mice.

DOG alleviated adipose tissue inflammation in HFD-challenged mice

HFD-induced obesity is accompanied with adipose tissue inflammation, resulting in elevated circulating inflammatory cytokines [26]. As shown in Fig. 2a–d, the serum levels of IL-1β, TNF-α, IL-6 and MCP-1 were increased in HFD-fed mice compared to those of the RD-fed mice, while high dosage of DOG treatment significantly decreased these cytokine levels in serum, and low dosage of DOG treatment only decreased the levels of IL-6 and MCP-1, when compared to those of the HFD-fed mice. Increased pro-inflammatory cytokines and elevated macrophage filtration are the main characteristics of adipose tissue inflammation. The infiltrated macrophages surround dead adipocytes to form crown-like structure, which is a typical characteristics of macrophage infiltration and adipose tissue inflammation. The H&E staining of eWAT sections from HFD-fed mice suggested bigger adipocytes and more infiltration of macrophages when compared with the RD-fed mice, which were obviously reversed by either high or low dosage of DOG treatment (Fig. 2e). The immunohistofluorescent staining of F4/80, a macrophage marker, and perilipin-1, a major coating protein of lipid droplets in adipocytes, further supported the above observation (Fig. 2f). Similarly, the cytokine levels in eWAT from HFD-fed mice, including IL-1β, TNF-α, IL-6 and MCP-1, were elevated, which were significantly abrogated by DOG treatment (Fig. 2g). The mRNA expression levels of IL-1β, TNF-α and IL-6 further supported the above results (Fig. 2h). These results suggested that DOG alleviates adipose tissue inflammation in HFD-induced obese mice by lessening macrophage infiltration.

DOG inhibits macrophage chemotaxis and mitigates pro-inflammatory polarization in eWAT from HFD-fed mice

MCP-1 and macrophage inflammatory protein-1α (MIP-1α) are the key chemokines for macrophage recruitment into adipose tissue [27]. The mRNA expression levels of chemokines for macrophage recruitment, including MCP-1, MIP-1α, C-C motif chemokine (Ccl) 5, Ccl11, C-X3-C-motif ligand 1 (Cx3cl1), C-X-C motif chemokine ligand 10 (Cxcl10), and chitinase 3-like protein 3 (Chi3l3), were markedly increased in eWAT from HFD-fed mice compared with RD-fed mice, and DOG treatment obviously suppressed the expression levels of these chemokines (Fig. 3a), indicating that DOG inhibited macrophage chemotaxis. To further confirm this hypothesis, a macrophage migration assay was performed using transwell system. When co-cultured with CM from fully differentiated 3T3-L1 adipocytes, the number of migrated THP-1 macrophages was significantly increased, when compared with the DMEM group, which was dose-dependently suppressed by pre-treatment with DOG (Fig. 3b, c). Moreover, HFD feeding was accompanied with increased expression of F4/80, CD11c (pro-inflammatory macrophage marker) and CD206 (anti-inflammatory macrophage marker) in eWAT, and high dosage of DOG treatment significantly reduced the expression of F4/80 and CD11c, and increased the expression of CD206, suggesting that DOG reversed HFD-induced pro-inflammatory polarization of macrophages in eWAT (Fig. 3d). Collectively, DOG mitigates adipose tissue inflammation by suppressing macrophage infiltration into eWAT and preventing pro-inflammatory polarization of macrophages in eWAT from HFD-fed mice.

DOG mitigates the abnormal deposition of extracellular matrix (ECM) components in eWAT

ECM components including collagen and fibronectin provide mechanical support for the physiological expansion of adipose tissue. However, the abnormal obesity-induced production and deposition of ECM leads to decreased tissue flexibility and the destruction of normal adipose tissue structure [28]. The Masson's trichrome staining and Sirius Red staining showed increased collagen deposition and the distinct pattern of collagen distribution in interstitial tissue of eWAT, and collagen fibers primarily formed in fibrotic bundles surrounding adipocytes in HFD-fed mice; interestingly, the abnormal deposition of collagen was attenuated by DOG treatment (Fig. 4a). Furthermore, the intense staining of α-smooth muscle actin (α-SMA) in the eWAT of HFD-induced obese mice indicated increased migration of activated myofibroblast-like cells into adipose tissue, leading to the secretion of more ECM components, and the intense staining of matrix metallopeptidase 9 (MMP-9) in the regions of macrophage-rich areas indicated that macrophages were involved in ECM component deposition (Fig. 4b). DOG inhibited the expression levels of ECM components including α-SMA and MMP-9, to protect against interstitial fibrosis (Fig. 4b). The above observation was further confirmed by Western blotting results (Fig. 4c). Taken together, these results suggested that DOG ameliorates abnormal ECM deposition in eWAT, which is conducive to the healthy expansion of adipose tissue.

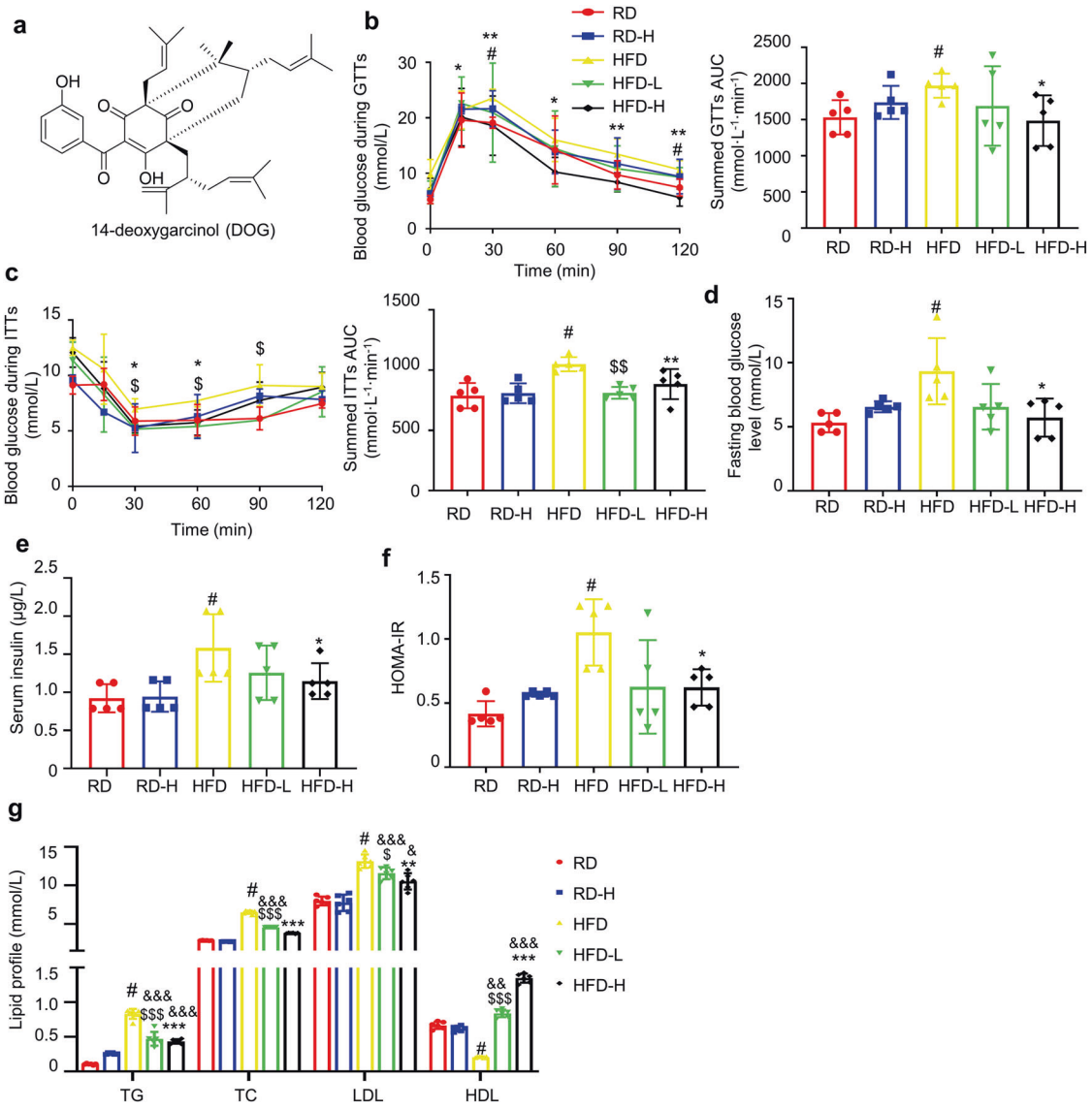

Fig. 1 DOG alleviates insulin resistance and hyperlipidemia in HFD-challenged mice. a Chemical structure of DOG. **b** Glucose tolerance test was performed after 2-week DOG treatment. AUC (area under curve) of each group was calculated. **c** Insulin tolerance test was performed after 3-week DOG treatment. AUC of each group was calculated. The blood glucose levels (**d**) and the serum insulin levels (**e**) of mice were determined after 16 h fasting. **f** The HOMA-IR index. **g** The lipid parameters in serum were measured. Data are expressed as means ± SEM. $n = 5$. $^{\#}P < 0.05$, HFD vs. RD; $^{\&}P < 0.05$, $^{\&\&}P < 0.01$, $^{\&\&\&}P < 0.001$, HFD-L, HFD-H vs. RD; $^{\$}P < 0.05$, $^{\$\$}P < 0.01$, $^{\$\$\$}P < 0.001$, HFD vs. HFD-L; $^{*}P < 0.05$, $^{**}P < 0.01$, $^{***}P < 0.001$, HFD vs. HFD-H.

DOG suppresses LPS plus nigericin-stimulated IL-1β secretion in THP-1 cells

As macrophage infiltration into adipose tissue was reduced in DOG treated mice, we hypothesized that DOG is able to mitigate inflammation in macrophages. Inhibition of NLRP3-caspase 1-mediated IL-1β production in macrophages plays a vital role in ameliorating adipose tissue inflammation [13]. Herein, LPS plus nigericin-stimulated THP-1 macrophages were recruited to evaluate the inhibitory effect of DOG against IL-1β secretion. DOG did not show obvious cytotoxicity on THP-1 macrophages up to 10 μM (Fig. 5a). DOG dose-dependently alleviated LPS plus nigericin-induced increase of IL-1β production and release, assessed by Western blotting and ELISA, respectively (Fig. 5b, c). As expected, DOG dose-dependently inhibited NLRP3 expression and caspase-1 activation in LPS plus nigericin-induced THP-1 macrophages (Fig. 5c). Consistently, the immunofluorescence staining results showed that NLRP3 and cleaved caspase 1 levels were largely decreased by DOG treatment in LPS plus nigericin-treated THP-1 cells (Fig. 5d, e). The NLRP3 inflammasome can be activated by not only nigericin but also extracellular ATP [29]. Thus, we further evaluated the inhibitory effect of DOG on LPS plus ATP-induced NLRP3 activation in THP-1 macrophages. The results showed that DOG suppressed the activation of NLRP3 and the release of IL-1β in LPS plus ATP-induced THP-1 cells (Supplementary Fig. S3). Taken together, DOG suppresses the activation of NLRP3 inflammasome in THP-1 macrophages, thus blocking the secretion of IL-1β.

DOG suppresses the activation of NF-κB signaling pathway in THP-1 cells

Since the NF-κB signaling pathway plays key roles in regulating inflammatory responses [30], we then evaluated the role of DOG in activation of NF-κB signaling pathway in THP-1 macrophages. As shown in Fig. 5f, LPS plus nigericin stimulation increased the phosphorylation levels of IKKα/β, IκBα, and p65, which was suppressed by the treatment of DOG. These results demonstrated that DOG suppresses the activation of NF-κB signaling

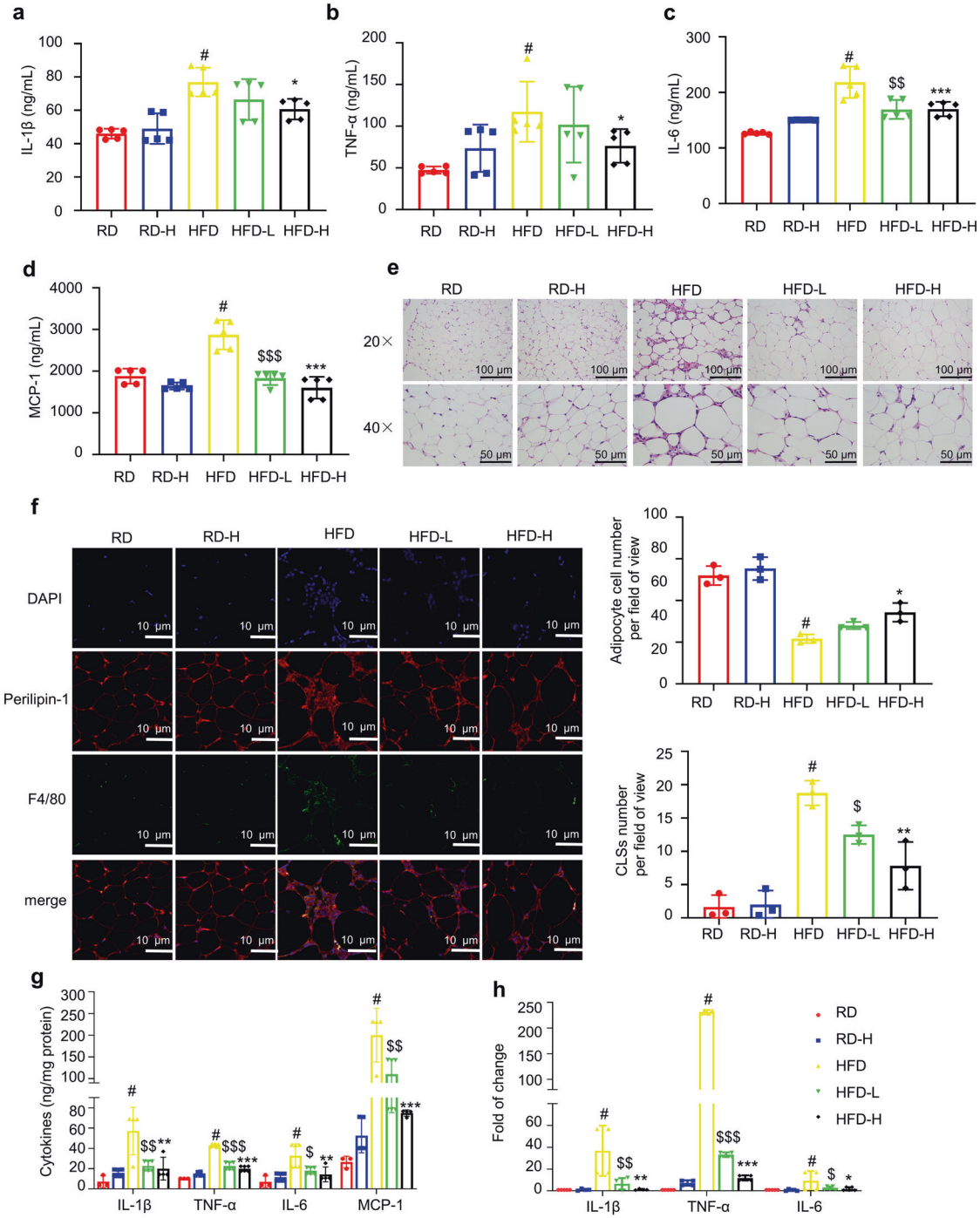

Fig. 2 DOG ameliorates HFD-induced adipose tissue inflammation in mice. The serum levels of IL-1β (**a**), TNF-α (**b**), IL-6 (**c**) and MCP-1 (**d**) were determined by ELISA kits. **e** Representative H&E staining images of eWAT. The number of adipocytes per field under 40× view in H&E-stained eWAT. **f** F4/80-positive staining in eWAT, scale bar = 10 μm. The number of CLSs per field of view was calculated using ImageJ software. **g** The levels of IL-1β, TNF-α, IL-6 and MCP-1 in eWAT were determined by ELISA kits. **h** The mRNA expression of IL-1β, TNF-α and IL-6 in eWAT. Data are expressed as means ± SEM. $n = 5$. $^{\#}P < 0.05$, HFD vs. RD; $^{\$}P < 0.05$, $^{\$\$}P < 0.01$, $^{\$\$\$}P < 0.001$, HFD vs. HFD-L; $^{*}P < 0.05$, $^{**}P < 0.01$, $^{***}P < 0.001$, HFD vs. HFD-H.

pathway to downregulate pro-IL-1β and NLRP3 expression in THP-1 macrophages.

DOG suppresses NLRP3 inflammasome activation through the deacetylase SIRT2

SIRT2, an NAD^{+}-dependent deacetylase, is a key metabolic sensor and inflammation regulator. Previous study indicated that SIRT2 directly deacetylates NLRP3 to modulate inflammatory responses and insulin sensitivity in aging mice [31]. Interestingly, LPS and nigericin stimulation decreased SIRT2 level, while DOG treatment increased SIRT2 expression in LPS and nigericin-induced THP-1 cells (Fig. 6a). LPS and nigericin treatment increased the acetylation level of NLRP3 in THP-1 cells, which was reversed by DOG treatment in a dose-dependent manner

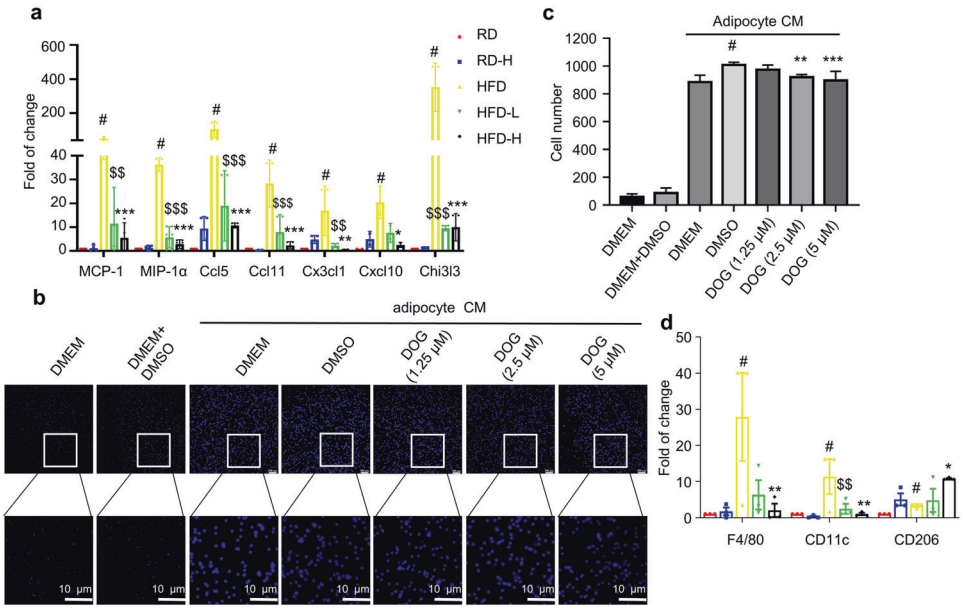

Fig. 3 DOG inhibits macrophage infiltration and pro-inflammatory polarization of macrophage in eWAT of obese mice. a The mRNA expression of MCP-1, MIP-1α, Ccl5, Ccl11, Cx3cl1, Cxcl10 and Chi3l3 in eWAT. $n = 5$. Fully differentiated 3T3-L1 adipocytes were treated with various concentrations of DOG for 12 h. Then, the cells were changed to fresh medium. After 24 h, the medium supernatants were collected as adipocyte CM. THP-1 macrophages were cultured in adipocyte CM for 4 h and the migrated THP-1 macrophages were visualized by DAPI staining (**b**) and quantified (**c**). Data are expressed as means ± SEM. $n = 3$. $^{\#}P < 0.05$, DMEM + DMSO vs. adipocyte CM + DMSO; $^{**}P < 0.01$, $^{***}P < 0.001$, adipocyte CM + DOG vs. adipocyte CM + DMSO. **d** The mRNA expression of F4/80, CD11c and CD206 in eWAT. Data are expressed as means ± SEM. $n = 5$. $^{\#}P < 0.05$, HFD vs. RD; $^{\$\$}P < 0.01$, $^{\$\$\$}P < 0.001$, HFD vs. HFD-L; $^{*}P < 0.05$, $^{**}P < 0.01$, $^{***}P < 0.001$, HFD vs. HFD-H.

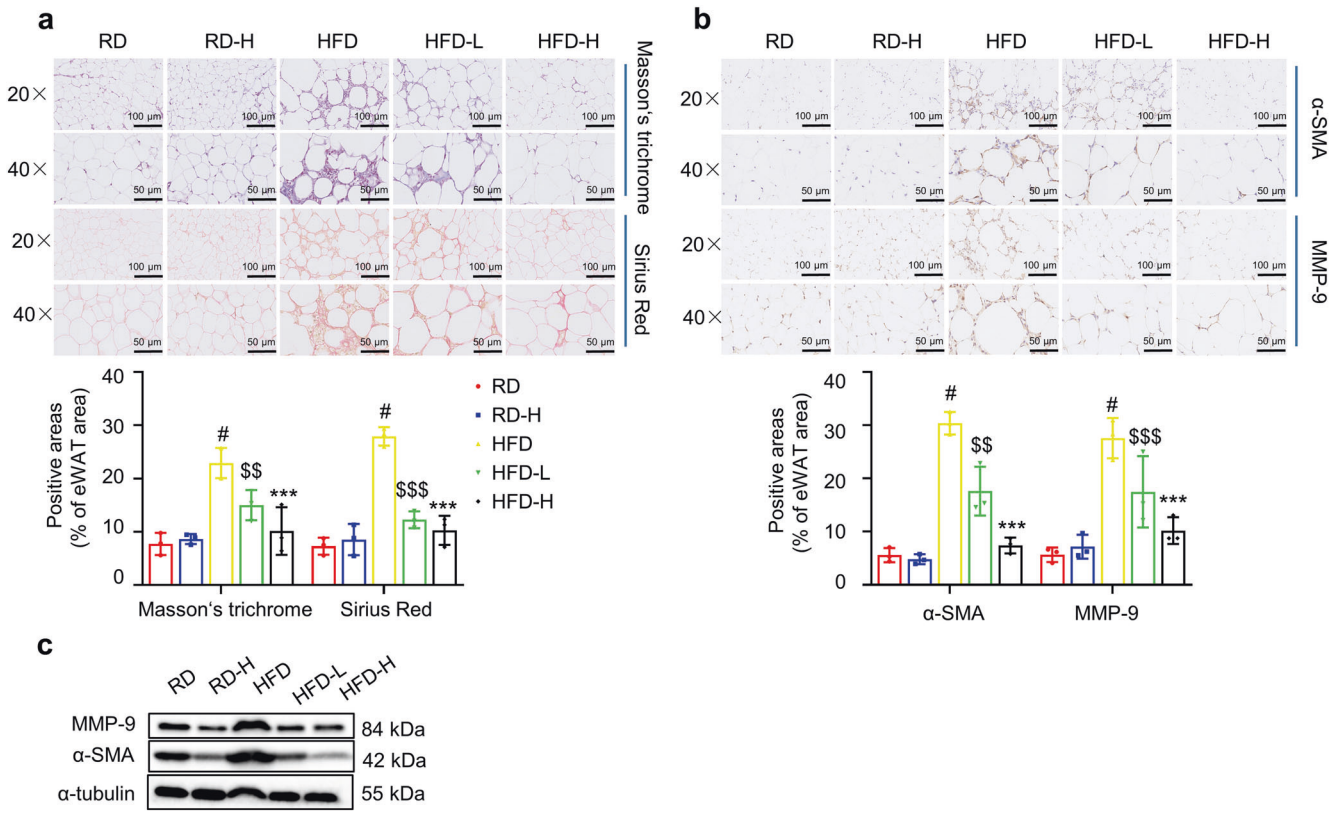

Fig. 4 DOG ameliorates abnormal ECM components in eWAT of HFD-challenged mice. a Representative images of Masson's trichrome staining (collagenous connective tissue fibers, blue-purple) and Sirius Red staining (collagen I/III fibers, pale pink) of eWAT. Original magnification, ×20 (top) and ×40 (bottom). The proportion of positive-stained areas to total areas in Masson's trichrome staining and Sirius Red staining of eWAT were estimated by ImageJ software. **b** Immunohistochemical staining of α-SMA and MMP-9 in eWAT. **c** The expression of MMP-9 and α-SMA in eWAT was detected by Western blotting. α-Tubulin was chosen as an internal loading control. Data are expressed as means ± SEM. $n = 3$. $^{\#}P < 0.05$, HFD vs. RD; $^{\$\$}P < 0.01$, $^{\$\$\$}P < 0.001$, HFD vs. HFD-L; $^{***}P < 0.001$, HFD vs. HFD-H.

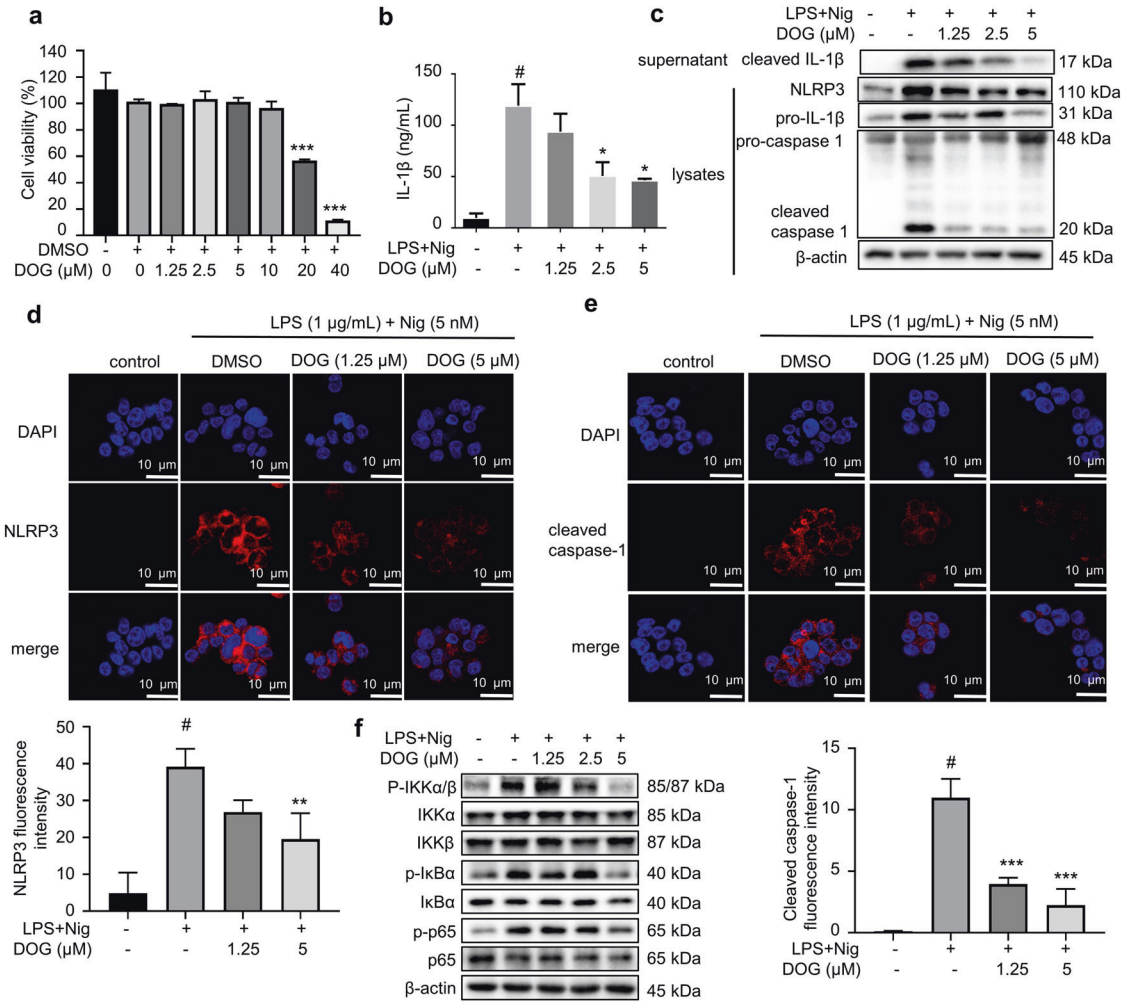

Fig. 5 DOG suppresses LPS plus nigericin-stimulated IL-1β secretion in THP-1 cells. a THP-1 cells were treated with different concentrations of DOG (from 1.25 to 40 μM) for 24 h. Cell viability was assessed by MTT assay ($n = 6$). THP-1 cells were cultured in the presence or absence of DOG for 12 h and stimulated with LPS for 4 h and then nigericin for 1 h. **b** The levels of IL-1β in the culture medium ($n = 3$). **c** The expression of NLRP3, pro-caspase 1, cleaved caspase 1, pro-IL-1β in the lysates, and cleaved IL-1β in the supernatant of THP-1 cells was detected by Western blotting. β-Actin was chosen as an internal loading control ($n = 3$). Immunofluorescence staining of NLRP3 (**d**) and cleaved caspase 1 (**e**). Scale bar = 10 μm. $n = 3$. **f** The protein levels of phospho-IKKα/β, IKKα, IKKβ, phospho-IκBα, IκBα, phospho-p65 and p65 were detected by Western blotting analyses. β-Actin was used as an internal loading control. $n = 3$. Data are expressed as means ± SEM. $^{\#}P < 0.05$, control vs. LPS + nigericin; $^{*}P < 0.05$, $^{**}P < 0.01$, $^{***}P < 0.001$ DOG vs. LPS + nigericin.

(Fig. 6b). Subsequently, CETSA was performed to confirm the interaction between DOG and SIRT2 deacetylase. Compared with the control cells, DOG treatment strongly stabilized SIRT2 at a series of temperatures from 50 to 90 °C (Fig. 6c). A selective SIRT2 inhibitor, AGK2, was used to confirm the effects of DOG [32]. DOG enhanced the SIRT2 deacetylating activity, which was totally abolished by the co-treatment of AGK2 (Fig. 6d). When co-treated with AGK2, the effects of DOG on increasing SIRT2 expression, and decreasing the acetylation level of NLRP3 and IL-1β secretion were almost blocked (Fig. 6e–g). Furthermore, co-treatment with AGK2 totally reversed the suppressing effect of DOG on NLRP3 activation and cleaved IL-1β in supernatants, assessed by Western blotting and immunofluorescence imaging (Fig. 6h, i). Consistently, the Western blotting results showed that NLRP3 and cleaved caspase 1 levels were largely decreased and SIRT2 expression was increased by DOG treatment in eWAT from HFD-fed mice (Supplementary Fig. S4). These results indicated that SIRT2 was a potential target involved in the suppressive effect of DOG against NLRP3 inflammasome activation.

DOG attenuates macrophage CM or TNF-α induced inflammatory responses in adipocytes

To further characterize the role of DOG in alleviating inflammatory responses in adipocytes, TNF-α-stimulated mature 3T3-L1 adipocytes were used. DOG did not show obvious cytotoxicity up to 10 μM in 3T3-L1 adipocytes (Fig. 7a). Compared with the vehicle cells, TNF-α treatment remarkably increased the secretion of NO, IL-1β, MCP-1 and IL-6 in adipocytes, whereas pre-treatment with DOG reversed the increases of these cytokines in dose-dependent manners (Fig. 7b–e). Consistently, the mRNA expression of IL-1β, IL-6 and iNOS was decreased in 3T3-L1 adipocytes treated with DOG (Fig. 7f). In addition, the TNF-α-induced increases of MCP-1, MIP-1α, Ccl5, Ccl11, Cx3cl1 and Cxcl10 mRNA expression were reversed by DOG supplementation (Fig. 7g), indicating that DOG inhibited macrophage chemotaxis. Furthermore, macrophage CM induced the secretion of IL-1β, MCP-1 and IL-6 in 3T3-L1 adipocytes, which was blocked by the pre-treatment of DOG in macrophages (Fig. 7h–j). These results indicated that DOG prevents TNF-α-induced inflammation and chemotaxis in adipocytes.

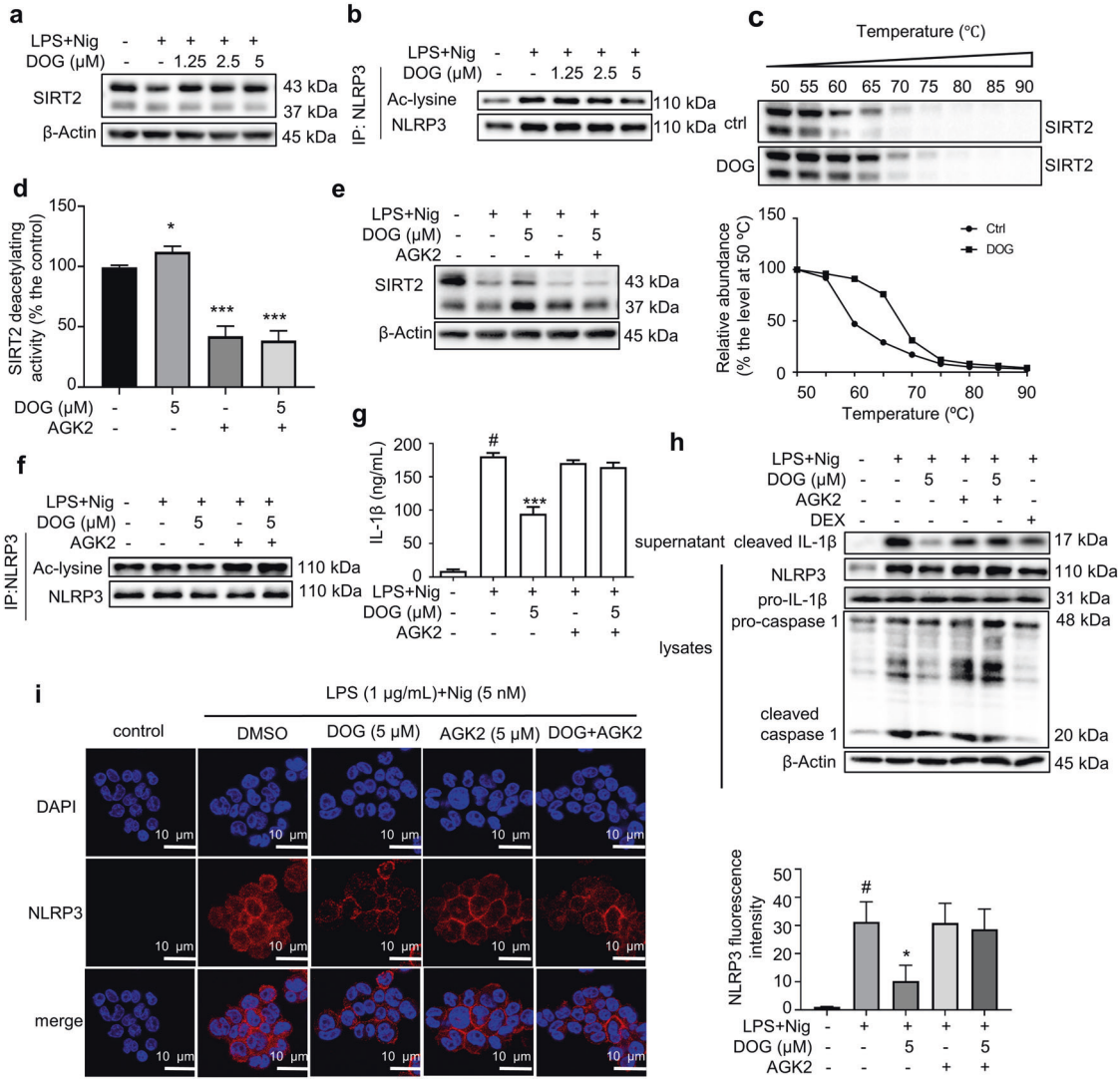

Fig. 6 DOG inhibits the activation of NLRP3 inflammasome through activating SIRT2. THP-1 cells were treated with various concentrations of DOG for 12 h, and then stimulated with LPS for 4 h and nigericin for 1 h. **a** The expression level of SIRT2 was detected by Western blotting ($n = 3$). β-Actin was chosen as an internal loading control. **b** The acetylated and total NLRP3 protein levels ($n = 3$). **c** CETSA was performed on THP-1 cells treated with or without DOG (5 μM) for 12 h ($n = 3$). **d** The effect of DOG or AGK2 on the deacetylating activity of SIRT2 ($n = 6$). THP-1 cells were treated with 5 μM DOG with or without 5 μM AGK2 for 12 h, and then stimulated with LPS for 4 h and nigericin for 1 h. **e** The expression level of SIRT2 was detected by Western blotting ($n = 3$). β-Actin was chosen as an internal loading control. **f** The acetylated and total NLRP3 protein levels ($n = 3$). **g** The levels of IL-1β in the culture medium from THP-1 cells ($n = 6$). **h** The expression of NLRP3, pro-caspase 1, cleaved caspase 1, and pro-IL-1β in the lysates, and cleaved IL-1β in the supernatant of THP-1 cells was detected by Western blotting ($n = 3$). β-Actin was chosen as an internal loading control. **i** Immunofluorescence staining of NLRP3. Scale bar = 10 μm. Data are expressed as means ± SEM. $^{\#}P < 0.05$, control vs. LPS + nigericin; $^{*}P < 0.05$, $^{***}P < 0.001$, DOG vs. LPS + nigericin.

DISCUSSION

Nowadays, brindle berry has been widely developed as herbal supplements to manage body weight; the main organic acid, hydroxycitric acid (HCA), is considered as the principle responsible for its anti-obese effect [33, 34]. Several randomized double-blind placebo-controlled clinical trials indicated that HCA is effective in humans in decreasing appetite, inhibiting fat synthesis, and reducing body weight [33]. Whereas other clinical studies indicated that HCA exerted no significant anti-obese effect as compared to the placebo group [35, 36]. Thus, the anti-obese principle of *G. cambogia* is still unclear. Garcinol and guttiferones K and M, three polyisoprenylated benzophenones isolated from *Garcinia* species, were reported to possess anti-inflammatory properties in LPS-treated macrophages, mainly through inhibiting NF-κB and/or Janus kinase/signal transducer and activator of transcription 1 activation [37–39]. DOG is a major polyisoprenylated benzophenone from the fruits of *G. cambogia*, which was found to inhibit NO production in LPS-stimulated RAW264.7 macrophages in our preliminary study. Herein, DOG was found to alleviate inflammatory responses in macrophages and adipocytes, and ameliorate adipose tissue inflammation in HFD-challenged obese mice. To the best of our knowledge, DOG is the first example of polyisoprenylated benzophenone to alleviate adipose tissue inflammation, which provides a novel scaffold for treating metabolic disorders.

Adipose tissue inflammation has been causally linked to obesity-associated insulin resistance and metabolic disorders [40]. In obese mice, the pro-inflammatory cytokines secreted from adipose tissue macrophages, including TNF-α, IL-1β, IL-6 and MCP-1, block insulin action in adipocytes, which provide a mechanistic link between inflammation and insulin

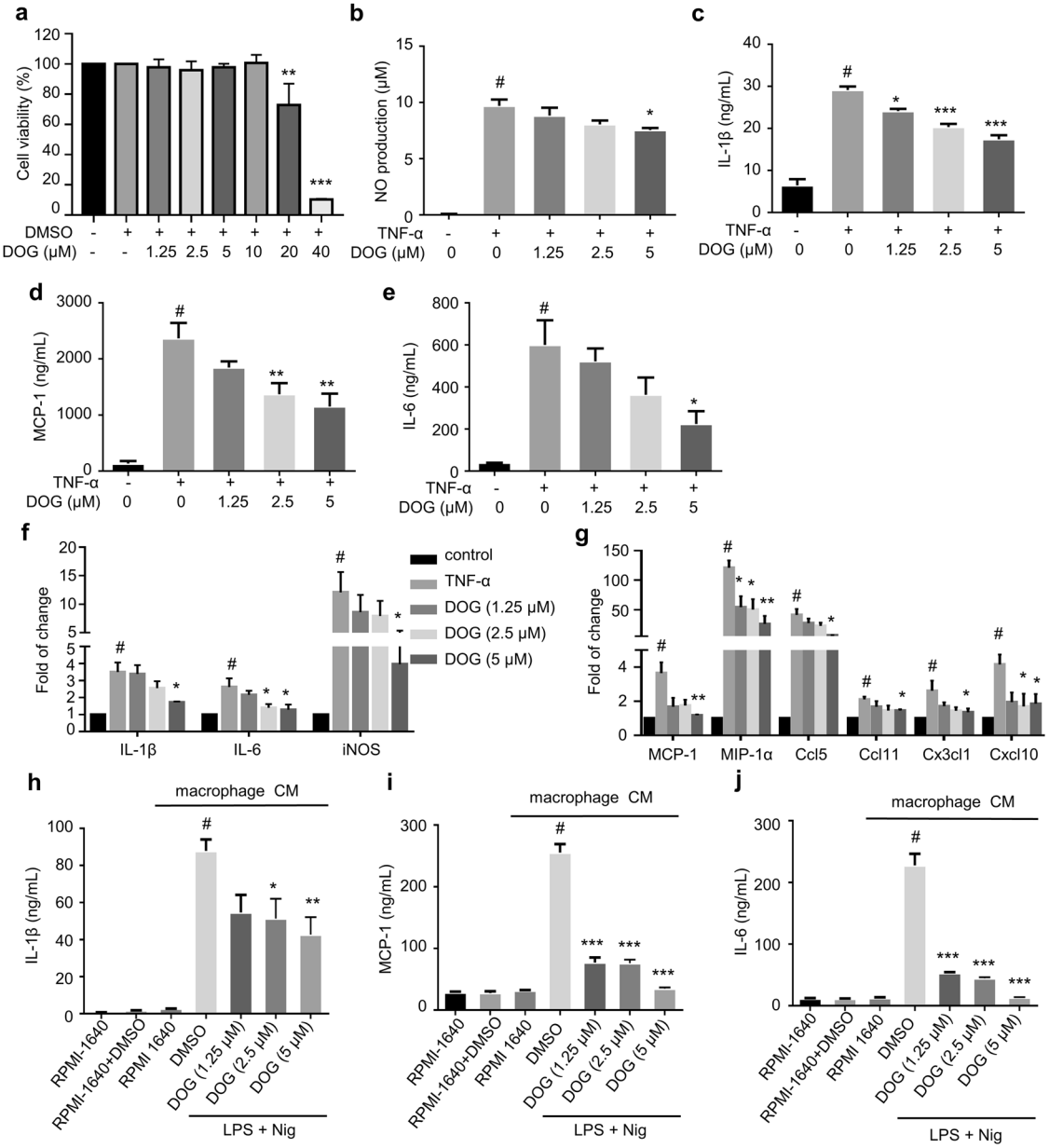

Fig. 7 DOG attenuates macrophage CM or TNF-α-induced inflammatory responses in adipocytes. a 3T3-L1 adipocytes were treated with different concentrations of DOG (from 1.25 to 40 μM) for 24 h. Cell viability was assessed by MTT assay. NO production (**b**) and the levels of IL-1β (**c**), MCP-1 (**d**) and IL-6 (**e**) in the culture medium from 3T3-L1 adipocytes were determined. **f** The mRNA expression of IL-1β, IL-6 and iNOS in 3T3-L1 adipocytes. **g** The mRNA expression of MCP-1, MIP-1α, Ccl5, Ccl11, Cx3cl1, and Cxcl10 in 3T3-L1 adipocytes. Data are expressed as means ± SEM. $n = 6$. $^{\#}P < 0.05$, control vs. TNF-α, $^{*}P < 0.05$, $^{**}P < 0.01$, $^{***}P < 0.001$, DOG vs. TNF-α. THP-1 cells were treated with 1.25, 2.5 or 5 μM DOG for 12 h. Subsequently, the cells were stimulated with LPS for 4 h and then nigericin for 1 h. Then, the cells were changed to fresh medium. After 24 h, the medium supernatants were collected as macrophage CM. The fully differentiated 3T3-L1 adipocytes were incubated in macrophage CM for 24 h. The levels of IL-1β (**h**), MCP-1 (**i**) and IL-6 (**j**) in 3T3-L1 adipocytes were determined. Data are expressed as means ± SEM. $n = 6$. $^{\#}P < 0.05$, RPMI-1640 + DMSO vs. macrophage CM + DMSO; $^{*}P < 0.05$, $^{**}P < 0.01$, $^{***}P < 0.001$, macrophage CM + DOG vs. macrophage CM + DMSO.

resistance [41, 42]. Numerous pro-inflammatory cytokines are secreted from WAT in genetically obese or diet-induced obese mice prior to the impairing of insulin signaling in adipocytes [43]. After infiltrating into adipose tissue, macrophages can differentiate into two phenotypes: pro-inflammatory M1 type and anti-inflammatory M2 type, which commonly referred as polarization [44, 45]. Accumulated evidence indicated that M1 macrophages are the major contributors of adipose tissue inflammation and insulin resistance in obese mice [7, 40, 46]. DOG obviously prevents macrophage infiltration and M1 macrophage polarization in eWAT to alleviate HFD-induced adipose tissue inflammation and systematic inflammation.

Under various pathological conditions, unresolved inflammation is often affiliated with altered tissue remodeling, and persistently inflammatory stress eventually evolves into fibrosis [47]. Fibrosis accumulation, characterized by excessive ECM component deposition in and around inflamed or damaged tissue, is considered to be a dysfunctional process in obesity and associated metabolic diseases [48]. ECM components such as collagen and fibronectin are necessary for tissue mechanical development, whereas the

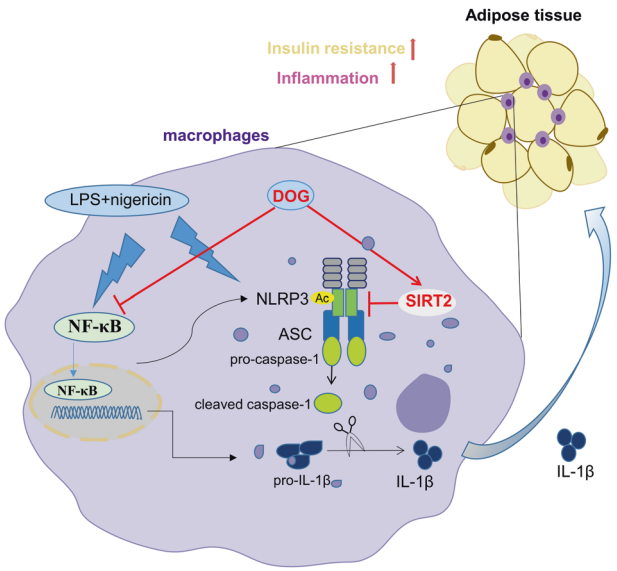

Fig. 8 Schematic models of DOG in attenuating adipose tissue inflammation. Therapeutically, DOG activates SIRT2 to suppress NF-κB/NLRP3 inflammasome-mediated IL-1β secretion, which in turn alleviates adipose tissue inflammation and improves insulin sensitivity.

obesity-associated excessive production and abnormal deposition of ECM components would gradually trigger the destruction of normal adipose tissue structure [28]. Consistently, the present study showed extensive interstitial fibrosis in the eWAT of HFD-induced obese mice. The decrease of fibrotic streaks together with the decreased markers of fibrosis indicated that DOG protects against HFD-induced remodeling in adipose tissue.

IL-1β plays an important role in the development of insulin resistance in murine and human adipocytes, which is elevated in adipose tissue of obese and insulin-resistant mice [49, 50]. In adipose tissue from obese subjects, the released level of IL-1β is comparable to that of TNF-α, which is originated from nonfat cells of adipose tissue [51]. In addition, IL-1β plays a pivotal role in regulating insulin levels and lipase activity under physiological conditions [52]. Furthermore, secreted IL-1β regulates the recruitment and activation of other immune cells, which further amplify the inflammatory response [53]. Thus, IL-1β possesses a permissive role in obesity-induced inflammation and insulin resistance. Inhibition of NLRP3-caspase 1-mediated IL-1β production in macrophages is positively related to the improvement of adipose tissue inflammation [13]. DOG effectively reduces the production and secretion of IL-1β in macrophages via the inhibition of NF-κB signaling pathway and NLRP3 inflammasome activation.

SIRT2 is one of the seven mammalian Sirtuins (SIRT1-SIRT7). SIRT2 participated in the regulation of adipocyte differentiation, gluconeogenesis, insulin sensitivity, and inflammatory responses through the deacetylation of specific substrates [54]. Moreover, SIRT2 is the most prominently expressed Sirtuin deacetylase in adipocytes [55, 56]. It has been reported that SIRT2 directly deacetylates and inactivates NLRP3 [31]. Our studies demonstrated that DOG increases the expression of SIRT2 and its deacetylating activity, which in turn inactivates NLRP3 inflammasome through SIRT2-mediated deacetylation of NLRP3.

Taken together, DOG alleviates adipose tissue inflammation by preventing macrophage recruitment and pro-inflammatory polarization in HFD-induced obese mice. Furthermore, DOG suppressed inflammatory responses in macrophages via reducing SIRT2-mediated NLRP3-dependent IL-1β secretion (Fig. 8). These findings suggested that DOG represents a novel drug candidate to regulate adipose tissue remodeling and treat insulin resistance and related metabolic abnormalities.

ACKNOWLEDGEMENTS

Financial support by National Natural Science Foundation of China (81872754), the Research Fund of University of Macau (MYRG2020-00091-ICMS), the Open Research Fund of Chengdu University of Traditional Chinese Medicine Key Laboratory of Systematic Research of Distinctive Chinese Medicine Resources in Southwest China, Internal Research Grant of the State Key Laboratory of Quality Research in Chinese Medicine, University of Macau (File No. QRCM-IRG2022-014), and the Science and Technology Development Fund, Macao SAR (File No. FDCT 0064/2021/AGJ) are gratefully acknowledged.

AUTHOR CONTRIBUTIONS

JLC conducted the experiments and drafted the manuscript; ZLF performed the isolation and identification of compounds and revised the manuscript. FZ and RHL conducted experiments and revised the manuscript. CP and YY supplied material and revised the manuscript. LGL conceived the study, designed the experiments, supplied financial support, and revised the manuscript. All the authors approved the final proof.

ADDITIONAL INFORMATION

Supplementary information The online version contains supplementary material available at https://doi.org/10.1038/s41401-022-00958-8.

Competing interests: The authors declare no competing interests.

Ethical approval: The procedures and operations involved in the animal experiments were performed according to the guidelines and regulations by the Animal Ethical and Welfare Committee of University of Macau (No. UMARE-033-2017). All animal experiments were carried out according to the guidelines of the National Institutes of Health (NIH) Guide for the Care and Use of Laboratory Animals. Male C57BL/6J mice (8–10 weeks old) were purchased from the animal facility of Faculty of Health Science, University of Macau (Macao, China). The mice were housed on a 12 h light-dark cycles at 22 ± 1 °C with a regular chow diet (Guangdong Medical Lab Animal Center, Guangzhou, China) and water *ad libitum* under standard conditions (specific-pathogen-free) with air filtration.

REFERENCES

1. World Health Organization. Obesity and overweight. 2021. https://www.who.int/news-room/fact-sheets/detail/obesity-and-overweight.
2. Chu DT, Minh Nguyet NT, Dinh TC, Thai Lien NV, Nguyen KH, Nhu Ngoc VT, et al. An update on physical health and economic consequences of overweight and obesity. Diabetes Metab Syndr. 2018;12:1095–100.
3. Smith GI, Mittendorfer B, Klein S. Metabolically healthy obesity: facts and fantasies. J Clin Invest. 2019;129:3978–89.
4. Lin K, Yang N, Luo W, Qian JF, Zhu WW, Ye SJ, et al. Direct cardio-protection of Dapagliflozin against obesity-related cardiomyopathy via NHE1/MAPK signaling. Acta Pharmacol Sin. 2022;43. https://doi.org/10.1038/s41401-022-00885-8. (In press).
5. Li D, Zhang T, Lu J, Peng C, Lin L. Natural constituents from food sources as therapeutic agents for obesity and metabolic diseases targeting adipose tissue inflammation. Crit Rev Food Sci Nutr. 2021;61:1947–65.
6. Li C, Xu MM, Wang K, Adler AJ, Vella AT, Zhou B. Macrophage polarization and meta-inflammation. Transl Res. 2018;191:29–44.
7. Wernstedt Asterholm I, Tao C, Morley TS, Wang QA, Delgado-Lopez F, Wang ZV, et al. Adipocyte inflammation is essential for healthy adipose tissue expansion and remodeling. Cell Metab. 2014;20:103–18.
8. Jo EK, Kim JK, Shin DM, Sasakawa C. Molecular mechanisms regulating NLRP3 inflammasome activation. Cell Mol Immunol. 2016;13:148–59.
9. Lawrence T. The nuclear factor NF-kappaB pathway in inflammation. Cold Spring Harb Perspect Biol. 2009;1:a001651.
10. Bauernfeind FG, Horvath G, Stutz A, Alnemri ES, MacDonald K, Speert D, et al. Cutting edge: NF-kappaB activating pattern recognition and cytokine receptors license NLRP3 inflammasome activation by regulating NLRP3 expression. J Immunol. 2009;183:787–91.
11. Abdul-Sater AA, Philpott DJ. Inflammasomes. In: Ratcliffe MJH, editor. Encyclopedia of immunobiology. Amsterdam: Academic Press; 2016. p 447–53.
12. Ehses JA, Lacraz G, Giroix MH, Schmidlin F, Coulaud J, Kassis N, et al. Il-1 antagonism reduces hyperglycemia and tissue inflammation in the type 2 diabetic gk rat. Proc Natl Acad Sci USA. 2009;106:13998–4003.
13. Vandanmagsar B, Youm YH, Ravussin A, Galgani JE, Stadler K, Mynatt RL, et al. The NLRP3 inflammasome instigates obesity-induced inflammation and insulin resistance. Nat Med. 2011;17:179–88.

14. Semwal RB, Semwal DK, Vermaak I, Viljoen A. A comprehensive scientific overview of *Garcinia cambogia*. Fitoterapia. 2015;102:134–48.
15. Raina R, Mondhe DM, Malik JK, Gupta RC. *Garcinia cambogia*. In: Gupta R, editor. Nutraceuticals. Amsterdam: Academic Press; 2016. p 669–80.
16. Jena BS, Jayaprakasha GK, Singh RP, Sakariah KK. Chemistry and biochemistry of (−)-hydroxycitric acid from *Garcinia*. J Agric Food Chem. 2002;50:10–22.
17. Koshy AS, Anila L, Vijayalakshmi NR. Flavonoids from *Garcinia cambogia* lower lipid levels in hypercholesterolemic rats. Food Chem. 2001;72:289–94.
18. Li L, Zhang H, Yao Y, Yang Z, Ma H. (-)-Hydroxycitric acid suppresses lipid droplet accumulation and accelerates energy metabolism via activation of the adiponectin-AMPK signaling pathway in broiler chickens. J Agric Food Chem. 2019;67:3188–97.
19. Feng Z, Chen J, Feng L, Chen C, Ye Y, Lin L. Polyisoprenylated benzophenone derivatives from *Garcinia cambogia* and their anti-inflammatory activities. Food Funct. 2021;12:6432–41.
20. Li D, Yang C, Zhu JZ, Lopez E, Zhang T, Tong Q, et al. Berberine remodels adipose tissue to attenuate metabolic disorders by activating sirtuin 3. Acta Pharmacol Sin. 2022;43:1285–98.
21. Van Dijk TH, Laskewitz AJ, Grefhorst A, Boer TS, Bloks VW, Kuipers F, et al. A novel approach to monitor glucose metabolism using stable isotopically labelled glucose in longitudinal studies in mice. Lab Anim. 2013;47:79–88.
22. Chen C, Ren YM, Zhu JZ, Chen JL, Feng ZL, Zhang T, et al. Ainsliadimer C, a disesquiterpenoid isolated from *Ainsliaea macrocephala*, ameliorates inflammatory responses in adipose tissue via Sirtuin 1-NLRP3 inflammasome axis. Acta Pharmacol Sin. 2022;43:1780–92.
23. Zhang T, Fang Z, Linghu KG, Li J, Gan L, Lin L. Small molecule-driven SIRT3-autophagy-mediated NLRP3 inflammasome inhibition ameliorates inflammatory crosstalk between macrophages and adipocytes. Br J Pharmacol. 2020;177:4645–65.
24. Shen S, Liao Q, Zhang T, Pan R, Lin L. Myricanol modulates skeletal muscle-adipose tissue crosstalk to alleviate high-fat diet-induced obesity and insulin resistance. Br J Pharmacol. 2019;176:3983–4001.
25. Shen S, Liao Q, Liu J, Pan R, Lee SM, Lin L. Myricanol rescues dexamethasone-induced muscle dysfunction via a sirtuin 1-dependent mechanism. J Cachexia Sarcopenia Muscle. 2019;10:429–44.
26. Hersoug LG, Moller P, Loft S. Role of microbiota-derived lipopolysaccharide in adipose tissue inflammation, adipocyte size and pyroptosis during obesity. Nutr Res Rev. 2018;31:153–63.
27. Shan B, Shao M, Zhang Q, Hepler C, Paschoal VA, Barnes SD, et al. Perivascular mesenchymal cells control adipose-tissue macrophage accrual in obesity. Nat Metab. 2020;2:1332–49.
28. Luo T, Nocon A, Fry J, Sherban A, Rui X, Jiang B, et al. AMPK activation by metformin suppresses abnormal extracellular matrix remodeling in adipose tissue and ameliorates insulin resistance in obesity. Diabetes. 2016;65:2295–310.
29. Sharif H, Wang L, Wang WL, Magupalli VG, Andreeva L, Qiao Q, et al. Structural mechanism for NEK7-licensed activation of NLRP3 inflammasome. Nature. 2019;570:338–43.
30. An Y, Zhang H, Wang C, Jiao F, Xu H, Wang X, et al. Activation of ROS/MAPKs/NF-kappaB/NLRP3 and inhibition of efferocytosis in osteoclast-mediated diabetic osteoporosis. FASEB J. 2019;33:12515–27.
31. He M, Chiang HH, Luo H, Zheng Z, Qiao Q, Wang L, et al. An acetylation switch of the NLRP3 inflammasome regulates aging-associated chronic inflammation and insulin resistance. Cell Metab. 2020;31:580–91.e5.
32. Outeiro TF, Kontopoulos E, Altmann SM, Kufareva I, Strathearn KE, Amore AM, et al. Sirtuin 2 inhibitors rescue α-synuclein–mediated toxicity in models of Parkinson's disease. Science. 2007;317:516–9.
33. Chuah LO, Ho WY, Beh BK, Yeap SK. Updates on antiobesity effect of *Garcinia* origin (-)-HCA. Evid Based Complement Altern Med. 2013;2013:751658.
34. Tomar M, Rao RP, Dorairaj P, Koshta A, Suresh S, Rafiq M, et al. A clinical and computational study on anti-obesity effects of hydroxycitric acid. RSC Adv. 2019;9:18578.
35. van Loon LJC, van Rooijen JJM, Niesen B, Verhagen H, Saris WHM, Wagenmakers AJM. Effects of acute (-)-hydroxycitrate supplementation on substrate metabolism at rest and during exercise in humans. Am J Clin Nutr. 2000;72:1445–50.
36. Heymsfield SB, Allison DB, Vasselli JR, Pietrobelli A, Greenfield D, Nunez C. *Garcinia cambogia* (hydroxycitric acid) as a potential antiobesity agent a randomized controlled trial. JAMA. 1998;280:1596–600.
37. Liao CH, Sang S, Liang YC, Ho CT, Lin JK. Suppression of inducible nitric oxide synthase and cyclooxygenase-2 in downregulating nuclear factor-kappa B pathway by garcinol. Mol Carcinog. 2004;41:140–9.
38. Chang NC, Yeh CT, Lin YK, Kuo KT, Fong IH, Kounis NG, et al. Garcinol attenuates lipoprotein(a)-induced oxidativestress and inflammatory cytokine production in ventricular cardiomyocyte through alpha7-nicotinic acetylcholine receptor-mediated inhibition of the p38 MAPK and NF-kappaB signaling pathways. Antioxidants. 2021;10:461.
39. Masullo M, Menegazzi M, Di Micco S, Beffy P, Bifulco G, Dal Bosco M, et al. Direct interaction of garcinol and related polyisoprenylated benzophenones of *Garcinia cambogia* fruits with the transcription factor STAT-1 as a likely mechanism of their inhibitory effect on cytokine signaling pathways. J Nat Prod. 2014;77:543–9.
40. Weisberg SP, McCann D, Desai M, Rosenbaum M, Leibel RL, Ferrante AW Jr. Obesity is associated with macrophage accumulation in adipose tissue. J Clin Invest. 2003;112:1796–808.
41. Wentworth JM, Naselli G, Brown WA, Doyle L, Phipson B, Smyth GK, et al. Pro-inflammatory $CD11c^{+}CD206^{+}$ adipose tissue macrophages are associated with insulin resistance in human obesity. Diabetes. 2010;59:1648–56.
42. Lumeng CN, Bodzin JL, Saltiel AR. Obesity induces a phenotypic switch in adipose tissue macrophage polarization. J Clin Invest. 2007;117:175–84.
43. Xu H, Barnes GT, Yang Q, Tan G, Yang D, Chou CJ, et al. Chronic inflammation in fat plays a crucial role in the development of obesity-related insulin resistance. J Clin Invest. 2003;112:1821–30.
44. Liu JQ, Zhao M, Zhang Z, Cui LY, Zhou X, Zhang W, et al. Rg1 improves LPS-induced Parkinsonian symptoms in mice via inhibition of NF-kappaB signaling and modulation of M1/M2 polarization. Acta Pharmacol Sin. 2020; 41:523–34.
45. Zhang Q, Chen LH, Yang H, Fang YC, Wang SW, Wang M, et al. GPR84 signaling promotes intestinal mucosal inflammation via enhancing NLRP3 inflammasome activation in macrophages. Acta Pharmacol Sin. 2021:s41401-021-00825-y.
46. Patsouris D, Li PP, Thapar D, Chapman J, Olefsky JM, Neels JG. Ablation of CD11c-positive cells normalizes insulin sensitivity in obese insulin resistant animals. Cell Metab. 2008;8:301–9.
47. Marcelin G, Silveira ALM, Martins LB, Ferreira AV, Clement K. Deciphering the cellular interplays underlying obesity-induced adipose tissue fibrosis. J Clin Invest. 2019;129:4032–40.
48. Wynn TA, Ramalingam TR. Mechanisms of fibrosis: therapeutic translation for fibrotic disease. Nat Med. 2012;18:1028–40.
49. Gao D, Madi M, Ding C, Fok M, Steele T, Ford C, et al. Interleukin-1beta mediates macrophage-induced impairment of insulin signaling in human primary adipocytes. Am J Physiol Endocrinol Metab. 2014;307:E289–304.
50. Nov O, Kohl A, Lewis EC, Bashan N, Dvir I, Ben-Shlomo S, et al. Interleukin-1beta may mediate insulin resistance in liver-derived cells in response to adipocyte inflammation. Endocrinology. 2010;151:4247–56.
51. Fain JN, Madan AK, Hiler ML, Cheema P, Bahouth SW. Comparison of the release of adipokines by adipose tissue, adipose tissue matrix, and adipocytes from visceral and subcutaneous abdominal adipose tissues of obese humans. Endocrinology. 2004;145:2273–82.
52. Matsuki T, Horai R, Sudo K, Iwakura Y. IL-1 plays an important role in lipid metabolism by regulating insulin levels under physiological conditions. J Exp Med. 2003;198:877–88.
53. Amir M, Czaja MJ. Inflammasome-mediated inflammation and fibrosis: it is more than just the IL-1beta. Hepatology. 2018;67:479–81.
54. Gomes P, Fleming Outeiro T, Cavadas C. Emerging role of Sirtuin 2 in the regulation of mammalian metabolism. Trends Pharmacol Sci. 2015;36:756–68.
55. Wang F, Nguyen M, Qin FX, Tong Q. SIRT2 deacetylates FOXO3a in response to oxidative stress and caloric restriction. Aging Cell. 2007;6:505–14.
56. North BL, Marshall BL, Borra MT, Denu JM, Verdin E. The human Sir2 ortholog, SIRT2, is an NAD^{+}-dependent tubulin deacetylase. Mol Cell. 2003; 11:437–44.